Melilite-Type Borates $Bi_2ZnB_2O_7$ and $CaBiGaB_2O_7$

Jacques Barbier,*,† Nicolas Penin,† and Lachlan M. Cranswick‡

Department of Chemistry, McMaster University, 1280 Main Street West, Hamilton, Ontario L8S4M1, Canada, and Neutron Program for Materials Research, National Research Council Canada, Chalk River Laboratories, Chalk River, Ontario K0J 1J0, Canada

Received February 10, 2005. Revised Manuscript Received April 21, 2005

The bismuth borates $Bi_2ZnB_2O_7$ and $CaBiGaB_2O_7$ have been synthesized by solid-state reactions at temperatures in the 650−825 °C range at 1 atm pressure. These compounds are the only synthetic diborate members of the melilite family, $A_2XZ_2O_7$, in which layers of A cations alternate with XZ_2O_7 tetrahedral layers. Except for $CdBiGaB_2O_7$, the synthesis of other substituted bismuth borate melilites has been unsuccessful. The crystal structures of $Bi_2ZnB_2O_7$ and $CaBiGaB_2O_7$ have been determined by powder X-ray diffraction and refined by the Rietveld method using powder neutron diffraction data. $CaBiGaB_2O_7$ adopts the regular tetragonal melilite structure ($P\bar{4}2_1m$ space group, $Z = 2$) containing B_2O_7 tetrahedral dimers. The refinement of split eight-coordinated sites for the Ca^{2+} and Bi^{3+} interlayer cations suggests the presence of additional disorder. $Bi_2ZnB_2O_7$ adopts a unique orthorhombic melilite superstructure (*Pba*2 space group, $Z = 4$) containing both tetrahedral B_2O_7 and triangular B_2O_5 dimers. The Bi^{3+} cations occupy two distinct interlayer sites with strongly asymmetric 6-fold coordination environments. The preliminary measurement of second harmonic generation efficiencies (d_{eff}) of powder samples has yielded values of 4.0 ($Bi_2ZnB_2O_7$) and 1.6 ($CaBiGaB_2O_7$) relative to a KH_2PO_4 standard.

Introduction

Binary bismuth borates have been of continuing interest for their optical properties,[1−4] in particular, the noncentrosymmetric BiB_3O_6 compound that displays a large nonlinear optical efficiency.[5−10] In contrast, only a handful of ternary bismuth borates have been reported in the literature: huntite-type $Bi(Fe_{1.35}Al_{1.65})(BO_3)_4$,[11] $Cu_5Bi_2B_4O_{14}$[12] recently characterized in detail, and three other compounds, viz., $Pb_4Bi_3B_7O_{19}$, $ZnBi_4B_2O_{10}$, and $CuBi_4B_2O_{10}$, only tentatively identified by powder X-ray diffraction.[13,14] We have therefore undertaken a more systematic survey of some $MO-Bi_2O_3-B_2O_3$ systems based on exploratory syntheses via solid-state reactions and crystal growth. These surveys have very recently led to the discovery of the novel noncentrosymmetric $BaBiBO_4$ compound.[15] The reinvestigation of the $ZnO-Bi_2O_3-B_2O_3$ system has now resulted in the discovery of yet another noncentrosymmetric compound, $Bi_2ZnB_2O_7$, which is closely related to the melilite structural family based on the åkermanite ($Ca_2MgSi_2O_7$) and gehlenite ($Ca_2Al_2SiO_7$) end-members. This paper describes the synthesis and crystal structure of $Bi_2ZnB_2O_7$, as well as those of its substituted derivatives, $CaBiGaB_2O_7$ and $CdBiGaB_2O_7$ (only unit-cell data are reported for the latter). Together with the okayamalite mineral, $Ca_2SiB_2O_7$,[16] these compounds are the only borate representatives of the melilite family known to date. Preliminary data on their nonlinear optical properties (efficiency for second harmonic generation) are briefly reported here as well. After completion of this work, a previous study[17] of the $Bi_2ZnB_2O_7$ compound was brought to our attention. However, to our knowledge, detailed results from this study have not been published in the literature.

Experimental Section

Solid-State Syntheses. The $Bi_2ZnB_2O_7$compound was discovered during the survey of the $ZnO-Bi_2O_3-B_2O_3$ system. Samples were synthesized via solid-state reactions from powder mixtures of Bi_2O_3 (Alfa Aesar, 99.975%), ZnO (Fisher Scientific, certified reagent, dried at 500 °C), and $B(OH)_3$ (Alfa Aesar, 99.99%). Small pellets

* Corresponding author. E-mail: barbier@mcmaster.ca.
† McMaster University.
‡ National Research Council Canada, Chalk River Laboratories.

(1) Becker, P.; Froehlich, R. *Z. Naturforsch. B* **2004**, *59*, 256.
(2) Filatov, S.; Shepelev, Y.; Bubnova, R.; Sennova, N.; Egorysheva, A. V.; Kargin, Y. F. *J. Solid State Chem.* **2004**, *177*, 515.
(3) Egorysheva, A. V.; Kanishcheva, A. S.; Kargin, Y. F.; Gorbunova, Y. E.; Mikhailov, Y. N. *Zh. Neorg. Khim.* **2002**, *47*, 1961.
(4) Muehlberg, M.; Burianek, M.; Edongue, H.; Poetsch, Ch. *J. Cryst. Growth* **2002**, *740*, 237−239.
(5) (a) Becker, P.; Liebertz, J.; Bohaty, L. *J. Cryst. Growth* **1999**, *203*, 149. (b) Becker, P.; Bohaty, L. *Cryst. Res. Technol.* **2001**, *36*, 1175.
(6) Kaminskii, A. A.; Becker, P.; Bohaty, L.; Ueda, K.; Takaichi, K.; Hanuza, J.; Maczka, M.; Eichler, H. J.; Gad, G. M. A. *Opt. Commun.* **2002**, *206*, 179.
(7) (a) Hellwig, H.; Liebertz, J.; Bohaty, L. *Solid State Commun*. **1999**, *109*, 249. (b) Hellwig, H.; Liebertz, J.; Bohaty, L. *J. Appl. Phys.* **2000**, *88*, 240.
(8) Lin, Z.; Wang, Z.; Chen, C.; Lee, M.-H. *J. Appl. Phys.* **2001**, *90*, 5585.
(9) Teng, B.; Wang, J.; Wang, Z.; Hu, X.; Jiang, H.; Liu, H.; Cheng, X.; Dong, S.; Liu, Y.; Shao, Z. *J. Cryst. Growth* **2001**, *233*, 282.
(10) Teng, B.; Wang, J.; Wang, Z.; Jiang, H.; Hu, X.; Song, R.; Liu, H.; Liu, Y.; Wei, J.; Shao, Z. *J. Cryst. Growth* **2001**, *224*, 280.
(11) Brixner, L. H.; Licis, M. S. *J. Solid State Chem*. **1971**, *3*, 172.
(12) Petrakovskii, G. A.; Vorotynov, A. M.; Sablina, K. A.; Udod, L. V.; Pankrats, A. I.; Ritter, C. J. *J. Magn. Magn. Mater*. **2003**, *263*, 245.
(13) (a) Shuster, N. S.; Zargarova, M. I.; Abdullaev, G. K. *Russ. J. Inorg. Chem*. **1985**, *30*, 1073. (b) Zargarova, M. I.; Kasumova, M. F.; Abdullaev, G. K. *Russ. J. Inorg. Chem*. **1987**, *32*, 737.
(14) Zargarova, M. I.; Mustafaev, N. M.; Shuster, N. S. *Inorg. Mater*. **1996**, *32*, 65.
(15) Barbier, J.; Penin, N.; Denoyer A.; Cranswick L. M. *Solid State Sci.* **2005**, in press.
(16) Giuli, G.; Bindi, L.; Bonazzi, P. *Am. Miner*. **2000**, *85*, 1512.
(17) Liebertz, J.; Wostrack, A.; Wirth, V.; Hellwig, H.; Held, P.; Bohatý, L. *Z. Kristallogr. Suppl*. **1997**, *12*, 185.

10.1021/cm0503073 CCC: $30.25
Published on Web 05/20/2005

Table 1. Unit-Cell Data for Melilite-Type Borates

	$Bi_2ZnB_2O_7$[a]	$CaBiGaB_2O_7$[a]	$CdBiGaB_2O_7$[b]	$Ca_2SiB_2O_7$[c]
symmetry	orthorhombic	tetragonal	tetragonal	tetragonal
space group	*Pba*2	$P\bar{4}2_1m$	$P\bar{4}2_1m$	$P\bar{4}2_1m$
a (Å)	10.8268(4)	7.4669(3)	7.4155(4)	7.1248(2)
b (Å)	11.0329(4)			
c (Å)	4.8848(2)	4.8344(2)	4.7933(5)	4.8177(2)
V (Å^3)	583.49	269.54	263.59	244.56
Z	4	2	2	2

[a] Powder neutron data (this work). [b] Powder X-ray data (this work). [c] Powder X-ray data for the okayamalite mineral (Giuli, G.; Bindi, L.; Bonazzi, P. *Am. Miner*. **2000**, *85*, 1542).

(0.5 g) were heated to 600−650 °C for 2−3 days in several stages with intermediate re-mixings. In all cases, care was taken to avoid any partial melting of the samples. These solid-state syntheses established that $Bi_2ZnB_2O_7$ is the only compound in the central region of the phase diagram and that $Bi_4ZnB_2O_{10}$ reported previously[13] does not exist. In fact, the X-ray powder pattern published for this hypothetical compound can be interpreted as a mixture of $Bi_2ZnB_2O_7$ and a cubic Bi_2O_3-rich sillenite-type phase. The unit-cell parameters of $Bi_2ZnB_2O_7$ are listed in Table 1 and its indexed X-ray powder pattern is given in Table 7 in the Supporting Information.

Following the characterization of $Bi_2ZnB_2O_7$ as a new member of the melilite series, the synthesis of other substituted derivatives was attempted. The two new compounds $CaBiGaB_2O_7$ and $CdBiGaB_2O_7$, corresponding to the double substitutions Bi^{3+} + tetrahedral $Zn^{2+} = Ca^{2+}/Cd^{2+}$ + tetrahedral Ga^{3+}, were successfully synthesized by solid-state reactions of stoichiometric mixtures of $CaCO_3$ (BDH inc. 99.0%) or CdO (Allied Chemicals, 98%), Bi_2O_3, Ga_2O_3 (Aldrich, 99.99%), and $B(OH)_3$ powders. Pellets (0.75 g) were slowly heated in stages up to 825 °C (Ca) or 650 °C (Cd) with several intermediate re-mixings. The maximum temperatures were chosen so as to avoid any partial melting of the samples. The formation of $CaBiGaB_2O_7$ and $CdBiGaB_2O_7$ was established via the indexing of their X-ray powder patterns (Tables 8 and 9 in the Supporting Information). Their unit-cell parameters are listed in Table 1. In the case of the Cd compound, a small amount of an unidentified phase was present in the product.

The attempted solid-state syntheses of the following melilites were unsuccessful: $Bi_2MB_2O_7$ (M = Be, Mg, Co), $MBiGaB_2O_7$ (M = Mg, Sr, Ba), $CaBiMB_2O_7$ (M = B, Al, In), and $MBiZnB_2O_7$ (M = Y, Nd, Yb). Either melting occurred at low temperature or other more stable borates formed. For instance, in the case of $ABiZnB_2O_7$ (A = Y, Nd, Yb), the only crystalline reaction products corresponded to the MBO_3 compounds.

Measurement of Nonlinear Optical Properties. The efficiency of second harmonic generation (SHG) in powder samples of $Bi_2ZnB_2O_7$ and $CaBiGaB_2O_7$ was evaluated using the Kurtz-Perry method.[18] About 50 mg of powder (particle size below 38 μm) was hand-pressed into a 7-mm-diameter pellet which was irradiated with a pulsed infrared beam (5 ns, 10 mJ, 10 Hz) produced by an optical parametric oscillator pumped by a Nd:YAG laser. A dichroic mirror was used to separate the signal from the fundamental and direct the visible light onto a photomultiplier. A combination of a half-wave achromatic retarder and a polarizer was used to control the intensity of the incident power (P_ω), which was measured with a fast IR photodiode. The intensity of the signal ($P_{2\omega}$) was fitted to $P_{2\omega} = Kd_{\text{eff}}^2P_\omega^2$. All the measurements were referred to a standard powder sample of KH_2PO_4 (KDP) considering that the factor *K* is nearly constant if the refractive indices and particle size of sample and reference are similar.

(18) Kurtz, S. K.; Perry, T. T. *J. Appl. Phys*. **1968**, *39*, 3798.

Table 2. Neutron Rietveld Refinements of the $Bi_2ZnB_2O_7$ and $CaBiGaB_2O_7$ Structures

	$Bi_2ZnB_2O_7$[a]	$CaBiGaB_2O_7$[a]
neutron wavelength (Å)	1.32995	1.32996
step size (deg)	0.1	0.1
2θ range (deg)	12.0−112.0	12.0−114.0[b]
no. of parameters	61	49
R_{wp}	0.070	0.081
R_{exp}	0.028	0.020[c]
χ^2	6.06	16.1[c]
R_{Bragg}	0.032	0.056
no. of reflections	659	198

[a] Unit-cell data are given in Table 1. [b] A few peaks from a trace impurity (maximum intensity of 11000 au) have been excluded from the refinement (Figure 1). [c] The lower R_{exp} and higher χ^2 indices are in part due to the higher counts for $CaBiGaB_2O_7$.

Structure Determinations and Refinements. A structure model for $Bi_2ZnB_2O_7$ was determined ab initio using X-ray powder diffraction data collected with a Guinier-Hägg camera using Cu $K\alpha_1$ radiation. The systematic absences observed in the X-ray powder pattern and in electron diffraction patterns recorded on microscopic single crystals were consistent with the *Pbam* or *Pba*2 space groups. The observation of a SHG signal generated from a powder sample led to the choice of the noncentrosymmetric *Pba*2 space group. The structure solution with four $Bi_2ZnB_2O_7$ formula units per unit cell was obtained with the FOX program[19] that easily revealed the melilite-type structure with layers of the heavy Bi^{3+} cations sandwiched between $ZnB_2O_7^{6-}$ layers. This structure type was also suggested by the compound stoichiometry and by the characteristic length of the *c* axis (~4.8 Å) corresponding to the layer stacking direction in melilites. The structure of $Bi_2ZnB_2O_7$ was subsequently refined by the Rietveld method using neutron powder data. For this purpose, a large (9 g) sample was synthesized by solid-state reaction as described above. ^{11}B-enriched boric acid (99.3% from Eagle-Picher) was used as a starting material in order to minimize the absorption of neutrons by the ^{10}B nuclei. The neutron diffraction data were collected at room temperature with the C2 high-resolution diffractometer at the Chalk River Laboratories. Details of the data collection and Rietveld refinement (with the FULLPROF program[20]) are summarized in Table 2 and the final Rietveld profile is shown in Figure 1. Atomic coordinates and displacement parameters are given in Table 3 and selected bond lengths and angles in Table 5.

The crystal structure of $CaBiGaB_2O_7$ was also refined by the Rietveld method using neutron diffraction data collected on a large (8 g) powder sample synthesized from ^{11}B-enriched boric acid. Based on its tetragonal unit cell, the initial model used for the refinement of $CaBiGaB_2O_7$ was the structure of gehlenite, $Ca_2Al_2SiO_7$, described in the $P\bar{4}2_1m$ space group with two formula units per unit cell.[21] In this model, the Ca^{2+} and Bi^{3+} cations were initially located on the same 4e site with *m* symmetry. Although unusual due to their very different coordination geometries, a similar Ca^{2+}/Bi^{3+} disorder has previously been observed, e.g., in $Ca_3Bi(PO_4)_3$,[22] $Ca_9Bi_3V_{11}O_{41}$,[23] and

(19) Favre-Nicolin, V. *FOX, Free Objects for Xtallography, version 1.6.0.2*., University of Geneva, Switzerland, 2003. See also Favre-Nicolin, V.; Cerny, R. *J. Appl. Crystallogr*. **2002**, *35*, 734. FOX uses a simulated annealing method for the ab initio solution of crystal stuctures by optimizing the positions and connectivity of known atoms, molecular fragments, or inorganic groups in the unit cell.

(20) Rodriguez-Carvajal, J. *FULLPROF.2k version 2.55*, 2004. Roisnel, T.; Rodriguez-Carvajal, J. *WinPLOTR* March 2004 version, Université de Rennes and Laboratoire Léon Brillouin, Saclay, France, 2004.

(21) Lejus, A. M.; Kahn-Harari, A.; Benitez, J. M.; Viana, B. *Mater. Res. Bull*. **1994**, *29*, 725.

(22) Barbier, J. *J. Solid State Chem*. **1992**, *101*, 249.

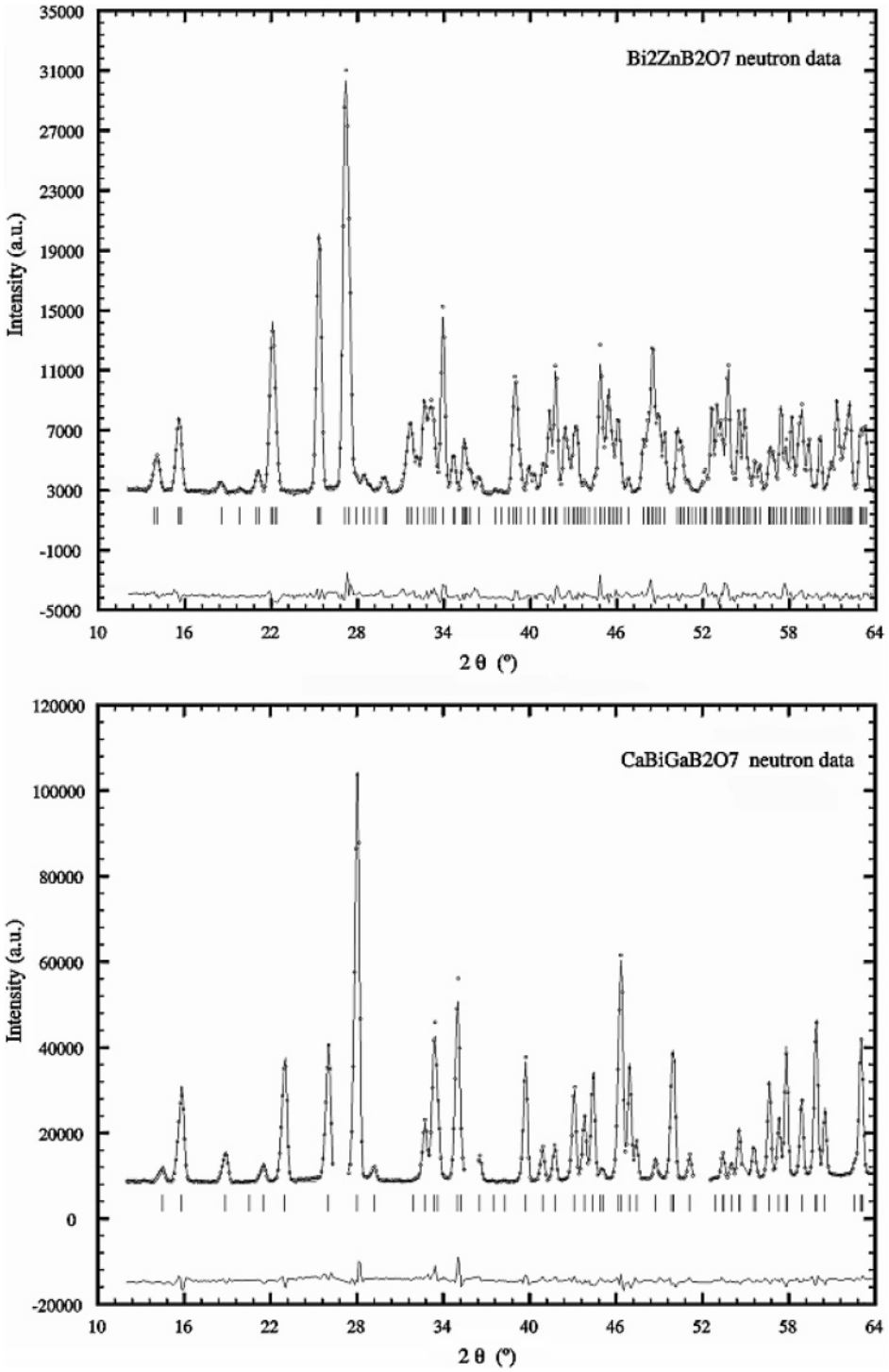

Figure 1. Final plots for the powder neutron Rietveld refinements of orthorhombic $Bi_2ZnB_2O_7$ (top) and tetragonal $CaBiGaB_2O_7$ (bottom). Only the low-angle regions ($2\theta = 10-64°$) are shown for clarity. The full profiles are available as Supporting Information. Very minor unindexed peaks (intensity < 11000 au) were excluded from the refinement of $CaBiGaB_2O_7$.

$Ca_4BiV_3O_{13}$.[24] After convergence of the refinement, rather large displacement parameters were obtained for all sites (e.g., $B = 1.49$ Å^2 for the Ca/Bi site), suggesting additional positional disorder or lower symmetry in the $CaBiGaB_2O_7$ structure. A refinement in the $P\bar{4}$ space group (subgroup of $P\bar{4}2_1m$) converged smoothly but also yielded a large displacement parameter for the Ca/Bi site ($B = 1.23$ Å^2) and generally larger esd's for atomic coordinates due to strong correlations. No indication was found in either neutron or X-ray diffraction data of a symmetry lower than tetragonal or of a larger unit cell that would allow Ca/Bi ordering, even in a sample slowly cooled from 800 to 350 °C at 3 °C/h. Eventually, a significant improvement of the refinement in $P\bar{4}2_1m$ was obtained after refining anisotropic displacement parameters and after splitting the Ca/Bi site by allowing the Bi^{3+} cation to shift off the mirror plane. Details of the data collection and Rietveld refinement (with the FULLPROF program) are summarized in Table 2 and the final Rietveld profile

(23) Radosavljevic, I.; Howard, J. A. K.; Sleight, A. W.; Evans, J. S. O. *J. Mater. Chem.* **2000**, *10*, 2091.
(24) Huang, J.-F.; Sleight, A. W. *J. Solid State Chem.* **1993**, *104*, 52.

Table 3. Atomic Coordinates and Displacement Parameters for $Bi_2ZnB_2O_7$ (Top) and $CaBiGaB_2O_7$ (Bottom)

	site	*x*	*y*	*z*	*B* (Å^2)
Bi1	4c	0.6812(4)	0.9666(4)	0.5770[a]	0.45(8)
Bi2	4c	0.4841(4)	0.6874(4)	0.5800(12)	0.39(8)
Zn	4c	0.2598(6)	0.7593(5)	0.0714(18)	0.32(10)
B1	4c	0.1150(5)	0.9802(5)	0.0818(18)	0.55(10)
B2	4c	0.5154(5)	0.8731(4)	0.1201(14)	0.43(10)
O1	4c	0.4141(6)	0.7997(6)	0.2513(18)	0.77(12)
O2	4c	0.1309(6)	0.6725(6)	0.2694(17)	0.59(12)
O3	4c	0.1946(6)	0.9149(5)	−0.0625(17)	0.53(11)
O4	4c	0.3008(6)	0.6737(6)	−0.2614(16)	0.55(11)
O5	4c	0.5197(6)	0.8583(5)	−0.1762(16)	0.67(12)
O6	2b	0.5	1.0	0.2119(19)	0.33(15)
O7	4c	0.1352(6)	1.0246(6)	0.3338(15)	0.57(13)
O8	2a	0.0	1.0	−0.0394(19)	0.54(15)

	site	*x*	*y*	*z*	U_{eq} (Å^2)	occupancy
Ca[b]	4e	0.1583(8)	0.6583(8)	0.4778(20)	0.0024(13)[c]	50%
Bi[b]	8f	0.1606(8)	0.6963(10)	0.5122(13)	0.0024(13)[c]	25%
Ga	2a	0.0	0.0	0.0	0.0100[d]	
B	4e	0.3679(3)	0.8679(3)	0.0475(5)	0.0252[d]	
O1	2c	0.5	0.0	0.1465(8)	0.0100[d]	
O2	4e	0.3554(3)	0.8554(3)	0.7558(6)	0.0156[d]	
O3	8f	0.0754(3)	0.1917(3)	0.7964(5)	0.0220[d]	

[a] *z*(Bi1) was used to fix the origin along *z*. [b] The Ca/Bi site is split with Bi displaced from the mirror plane. [c] Common isotropic displacement parameter. [d] Anisotropic displacement parameters were refined (Table 4).

is shown in Figure 1. Atomic coordinates and displacement parameters are given in Tables 3 and 4 and selected bond lengths and angles in Table 6.

Results and Discussion

Description of the $CaBiGaB_2O_7$ Structure. The $CaBiGaB_2O_7$ compound crystallizes with the noncentrosymmetric tetragonal melilite structure-type, with $P\bar{4}2_1m$ symmetry and two formula units per unit cell. Corner-sharing GaO_4 tetrahedra and B_2O_7 tetrahedral dimers form (001) layers interleaved with layers of Ca^{2+} and Bi^{3+} cations (Figure 2). The GaO_4 tetrahedra are quasi-regular by symmetry whereas the BO_4 tetrahedra show distortions in bond lengths and bond angles (Table 6). The spread of B−O distances is in qualitative agreement with bond valence arguments that predict a shorter B−O2 bond (viz., B−O1 = 1.50 Å, B−O2 = 1.41 Å, B−O3 = 1.51 Å, as calculated by the Bond Valence Wizard program[25]). As a result of the splitting of the Ca^{2+} and Bi^{3+} positions, both cations achieve a proper bond valence sum. The 8-fold coordination of the Bi^{3+} cation is unusual but its shift to a general position off the mirror plane yields an asymmetrical coordination with three shorter Bi−O bonds (2.22−2.39 Å), in agreement with the effect expected from a stereoactive lone pair. The Ca/Bi splitting along the *z* direction is also associated with a significant anisotropy of some of the displacement parameters (e.g., U_{33} for O3 in Table 4), which could indicate the presence of additional disorder or of a modulation in the $CaBiGaB_2O_7$ structure. The $P\bar{4}2_1m$ symmetry clearly only describes an average structure and the growth of single crystals will be attempted in order to investigate this point further.

Description of the $Bi_2ZnB_2O_7$ Structure. The $Bi_2ZnB_2O_7$ compound is a noncentrosymmetric orthorhombic derivative of the melilite structure type with the following symmetry relationship: tetragonal melilite ($P\bar{4}2_1m$, *a*, *c*, *Z* = 2) → hypothetical orthorhombic derivative (*Cmm*2, subgroup of $P\bar{4}2_1m$, type I, $\sim a\sqrt{2}$, $\sim a\sqrt{2}$, *c*, *Z* = 4) → orthorhombic $Bi_2ZnB_2O_7$ (*Pba*2, subgroup of *Cmm*2, type IIa, $\sim a\sqrt{2}$, $\sim a\sqrt{2}$, *c*, *Z* = 4). The structure consists of (001) $ZnB_2O_7^{6-}$ layers alternating with layers of Bi^{3+} cations (Figure 3). Unlike okayamalite ($Ca_2SiB_2O_7$) where all B atoms are tetrahedrally coordinated, the borate layers in $Bi_2ZnB_2O_7$ contain both tetrahedral B_2O_7 and triangular B_2O_5 diborate groups. Their alternating arrangement in the *a* and *b* directions, the tilting of the ZnO_4 tetrahedra, and the positions of the Bi^{3+} cations all contribute to the formation of the ($\sim a\sqrt{2}$, $\sim a\sqrt{2}$, *c*) superstructure. The Bi^{3+} cations occupy two distinct sites, both asymmetrically six-coordinated with three short Bi−O bonds in the range of 2.14−2.31 Å (Table 5). All bond valence sums are close to their expected values. It is noteworthy that the triangular coordination around the B1 atom in the B_2O_5 groups is ideally planar with a sum of O−B1−O bond angles equal to 360°. The formation of these B_2O_5 groups can be seen as a result of the asymmetrical coordination around the Bi^{3+} cations as imposed by the presence of their stereoactive lone pairs: the two shortest Bi1−O4 (2.17 Å) and Bi2−O4 (2.14 Å) bonds prevent the O4 atom from approaching the B1 atom (B1···O4 = 2.87 Å) and preclude the formation of tetrahedral B_2O_7 groups around B1 (Figure 3). Alternatively, the B_2O_5 groups could be seen as the product of an extreme displacive transformation in which the formation of two Bi−O4 bonds is favored over that of one B−O4 bond.

Occurrence of Borate Melilites. The borates described here, $Bi_2ZnB_2O_7$, $CaBiGaB_2O_7$, and $CdBiGaB_2O_7$, belong to the large family of natural and synthetic melilites, $A_2XZ_2O_7$, in which A cations (Na, Ca, Sr, Ba, Cd, Pb, Y, Ln) are interleaved between XZ_2O_7 tetrahedral layers (X = Be, Mg, Co, Fe, Mn, Cu, Zn, Cd, Al, Ga; Z = Be, B, Al, Ga, Si, Ge). Melilites have been investigated extensively in the past and are still of current interest for their crystal chemical properties (e.g., $Ca_2CoSi_2O_7$[26]) as well as their potential applications as laser host materials (e.g., $Y_2SiBe_2O_7$[27] or $SrLaGa_3O_7$[28]). These studies have shown that the predominant crystal chemical factor influencing the stability of the melilite structure is the size misfit between the tetrahedral layers and the interlayer cations.[29−31] In that regard, it is noteworthy that only one other diborate melilite is known, viz. $Ca_2SiB_2O_7$, occurring as the rare mineral okayamalite[16] and as a metastable synthetic compound obtained by dehydration of the mineral datolite, $CaBSiO_4OH$.[32] The mean size of the SiB_2O_7 tetrahedral layer is clearly the smallest among all melilites and is apparently only able to accom-

(25) Orlov, I. P. *Bond Valence Wizard, version 2.01*, École Polytechnique Fédérale de Lausanne, Switzerland, 2002. See also Orlov. I. P.; Popov, K. A.; Urusov, V. S. *J. Struct. Chem.* **1998**, *39*, 575.

(26) Hagiya, K.; Kusaka, K.; Ohmasa, M.; Iishi, K. *Acta Crystallogr. B* **2001**, *57*, 271.

(27) Kuz'micheva, G. M.; Rybakov, V. B.; Kutovoi, S. A.; Panyutin, V. L.; Oleinik, A. Yu.; Plashkarev, O. G. *Inorg. Mater.* **2002**, *38*, 60.

(28) Kaczmarek, S. M.; Boulon, G. *Opt. Mater.* **2003**, *24*, 151.

(29) Seifert, F. *N. Jb. Miner. Mh.* **1986**, *1*, 8.

(30) Röthlisberger, F.; Seifert, F.; Czank, M. *Eur. J. Mineral.* **1990**, *2*, 585.

(31) Mill, B. V.; Baibakova, G. D. *Russ. J. Inorg. Chem.* **1990**, *35*, 341.

(32) Tarney, J.; Nicol, A. W.; Marriner, G. F. *Miner. Mag.* **1973**, *39*, 158.

Table 4. Anisotropic Displacement Parameters for $CaBiGaB_2O_7$

	U_{11}	U_{22}	U_{33}	U_{12}	U_{13}	U_{23}	U_{eq} (Å^2)
Ga	0.0039(4)	0.0039(4)	0.0069(13)	0.0	0.0	0.0	0.0100
B	0.0106(4)	0.0106(4)	0.0133(15)	−0.0039(5)	−0.0048(5)	−0.0048(5)	0.0252
O1	0.0038(5)	0.0038(5)	0.0074(19)	0.0006(8)	0.0	0.0	0.0100
O2	0.0063(4)	0.0063(4)	0.0097(14)	−0.0018(5)	−0.0000(7)	−0.0000(7)	0.0156
O3	0.0062(4)	0.0070(5)	0.0245(58)	0.0018(4)	0.0027(7)	0.0058(6)	0.0220

Table 5. Selected Bond Distances (Å), Bond Valences (s), and Bond Angles (°) in $Bi_2ZnB_2O_7$

		s^a			s^a
Bi1−O4	2.168(7)	0.810	Zn−O4	1.932(10)	0.540
Bi1−O2	2.216(8)	0.711	Zn−O1	1.939(9)	0.530
Bi1−O7	2.318(7)	0.540	Zn−O2	1.949(9)	0.516
Bi1−O5	2.437(8)	0.391	Zn−O3	1.968(8)	0.490
Bi1−O3	2.572(8)	0.272		Σ*s*	2.08
Bi1−O6	2.677(7)	0.205	B1−O3	1.326(9)	1.129
	Σ*s*	2.93	B1−O7	1.343(11)	1.079
Bi2−O4	2.136(8)	0.883	B1−O8	1.395(7)	0.937
Bi2−O1	2.165(9)	0.817		Σ*s*	3.14
Bi2−O5	2.263(8)	0.627	B2−O1	1.507(9)	0.692
Bi2−O7	2.519(8)	0.314	B2−O5	1.457(10)	0.793
Bi2−O2	2.686(8)	0.200	B2−O6	1.479(6)	0.747
Bi2−O8	2.786(8)	0.152	B2−O2	1.532(8)	0.647
	Σ*s*	2.99		Σ*s*	2.88

O1−Zn−O2	120.3(6)	O3−B1−O7	125.4(10)
O1−Zn−O3	105.0(6)	O3−B1−O8	116.1(7)
O1−Zn−O4	107.2(7)	O7−B1−O8	118.5(9)
O2−Zn−O3	109.7(6)	O1−B2−O2	102.4(7)
O2−Zn−O4	110.0(7)	O1−B2−O5	112.7(9)
O3−Zn−O4	103.2(6)	O1−B2−O6	107.3(6)
		O2−B2−O5	114.2(9)
		O2−B2−O6	105.0(5)
		O5−B2−O6	114.2(8)

[a] Bond valence parameters from Brese, N. E.; O'Keeffe, M. *Acta Crystallogr. B* **1991**, *47*, 192.

Table 6. Selected Bond Distances (Å), Bond Valences (s), and Bond Angles (°) in $CaBiGaB_2O_7$

		s^a			s^a
Ca−O3 ×2	2.402(8)	0.309	Ga−O3 ×4	1.826(2)	0.771
Ca−O1	2.469(9)	0.257		Σ*s*	3.08
Ca−O2	2.477(8)	0.252	B−O2	1.416(4)	0.885
Ca−O2 ×2	2.531(7)	0.218	B−O1	1.475(3)	0.755
Ca−O3 ×2	2.583(8)	0.189	B−O3 ×2	1.574(3)	0.578
	Σ*s*	1.94		Σ*s*	2.80
Bi−O2	2.217(7)	0.709	O3−Ga−O3	106.9(2) ×4	
Bi−O3	2.277(7)	0.603	O3−Ga−O3	114.8(2) ×2	
Bi−O3	2.386(7)	0.449	O1−B−O2	114.3(3)	
Bi−O3	2.472(7)	0.356	O1−B−O3	102.9(2) ×2	
Bi−O1	2.512(7)	0.320	O2−B−O3	116.1(3) ×2	
Bi−O2	2.650(7)	0.220	O3−B−O3	102.7(3)	
Bi−O3	2.687(7)	0.199			
Bi−O2	2.859(7)	0.125			
	Σ*s*	2.98			

[a] Bond valence parameters from Brese, N. E.; O'Keeffe, M. *Acta Crystallogr. B* **1991**, *47*, 192.

modate the relatively small Ca^{2+} cation. Consequently, okayamalite crystallizes with a very small unit cell (Table 1). As expected, the substitution of Ga or Zn for Si leads to a larger unit cell with an anisotropic in-plane expansion of the tetrahedral layers. For instance, from $Ca_2SiB_2O_7$ to $CaBiGaB_2O_7$, the *c* and *a* axes expand by 0.3% and 4.8%, respectively (Table 1). The minor change in the *c* axis reflects the similar effective sizes of the interlayer Ca^{2+} and Bi^{3+} cations.

Despite the straightforward syntheses of $CaBiGaB_2O_7$ and $Bi_2ZnB_2O_7$, no previous report of Bi-substituted melilites could be found in the literature. $Bi_2ZnB_2O_7$ itself is unique among melilites in several respects: first, it is the only known example in which the layers contain triangular B_2O_5 groups, a structural feature that obviously can only be found in borate melilites; second, it is the only melilite structure in which the interlayer cations occupy two crystallographically distinct sites; and third, as a result of the unique structural arrangement within and between the layers, it is the only melilite to crystallize with a fully ordered, commensurate superstructure with *Pba2* symmetry. The same space group symmetry would be expected from cation ordering in other melilites containing two different interlayer cations, such as $MLnT_3O_7$ (M = Ca, Sr, Ba; Ln = lanthanide; T = Al, Ga), but it has not been reported so far. As described above, the formation of B_2O_5 groups in the $Bi_2ZnB_2O_7$ structure occurs in synergy with the asymmetrical bonding requirement of the Bi^{3+} cations, suggesting that the latter could stabilize other $Bi_2XB_2O_7$ diborate melilites. Our own attempts with X = Mg^{2+} and Co^{2+} (with ionic radii similar to that of Zn^{2+}) have been unsuccessful possibly because the tetrahedral coordination of these particular cations is not favored at the relatively low synthesis temperatures required to avoid the melting of borate melilites. Similar difficulties may be anticipated for the synthesis of other hypothetical melilites, such as $Bi_2FeB_2O_7$, $Bi_2MnB_2O_7$, and $Bi_2CuB_2O_7$. The possible existence of $Bi_2CdB_2O_7$ remains to be investigated.

Attempts to substitute Bi^{3+} in $Bi_2ZnB_2O_7$ with other trivalent cations of similar size have also been unsuccessful. For example, the $Y_2ZnB_2O_7$, $BiNdZnB_2O_7$, or $BiYbB_2O_7$ melilites could not be synthesized and the simple MBO_3 orthoborates formed instead. This result suggests that the formation of $Bi_2ZnB_2O_7$ itself could be favored by the metastable nature of $BiBO_3$.[1]

Double substitutions in $Bi_2ZnB_2O_7$ have been successful for $Bi^{3+} + Zn^{2+} = Ca^{2+}$ (or Cd^{2+}) + Ga^{3+}, as described above. This result is consistent with the influence of the $\langle r_T\rangle/\langle r_A\rangle$ size ratio on the stability of $A_2T_3O_7$ melilites:[29] the ratios for $CaBiGaB_2O_7$ (0.29) and $CdBiGaB_2O_7$ (0.29) are indeed close to that for $Bi_2ZnB_2O_7$ (0.31) (using Shannon's ionic radii [33] with C.N. = 8 for the A cations and C.N. = 4 for the T cations). On the other hand, hypothetical melilites with similar ratios, such as $CaBiAlB_2O_7$ (0.26), $CaBiFeB_2O_7$ (0.29), and $SrBiGaB_2O_7$ (0.27), could not be synthesized. Although the melilite structure is known to accommodate a large range of $\langle r_T\rangle/\langle r_A\rangle$ ratios (e.g., from 0.32 in $Ca_2BeSi_2O_7$ to 0.48 in $Ca_2ZnGe_2O_7$ and $CaLaGa_3O_7$), it is clear that borate melilites lie at the lower limit of this range and that, consequently, other factors may become predominant in determining their stability. For example, the attempted syntheses of $CaBiFeB_2O_7$ and $SrBiGaB_2O_7$ yielded mixtures containing the two novel compounds $MBi_2B_2O_7$ (M = Ca,

(33) Shannon, R. D. *Acta Crystallogr. A* **1976**, *32*, 751.

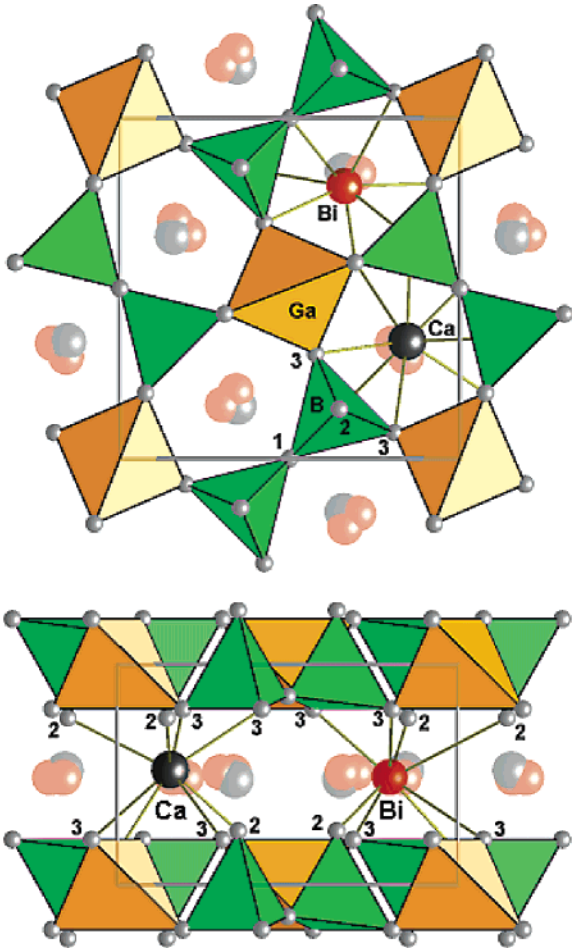

Figure 2. Structure of tetragonal $CaBiGaB_2O_7$ viewed along the [001] (top) and [100] (bottom) directions. The Ca and Bi positions are half-filled and the Bi positions are split across the mirror planes. Numbers correspond to the oxygen positions in Table 3.

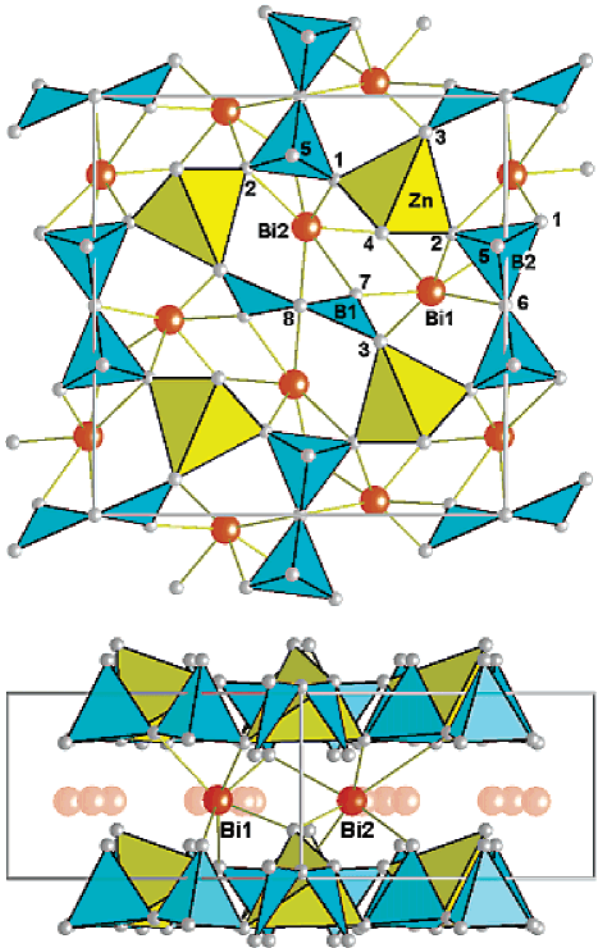

Figure 3. Structure of orthorhombic $Bi_2ZnB_2O_7$ viewed along the [001] (top) and [1−10] (bottom) directions. Numbers correspond to the oxygen positions in Table 3.

Sr) instead of the melilites. The characterization of these novel bismuth borates is in progress.

Nonlinear Optical Properties. Only one preliminary measurement of the efficiency for second harmonic generation (SHG) of $Bi_2ZnB_2O_7$ and $CaBiGaB_2O_7$ has been carried out by the Kurtz-Perry method using powder samples. In agreement with their noncentrosymmetric crystal structures, both compounds produced an SHG signal with efficiencies (d_{eff}) equal to 4.0 ($Bi_2ZnB_2O_7$) and 1.6 ($CaBiGaB_2O_7$) relative to a KH_2PO_4 standard of similar grain size. The larger efficiency for $Bi_2ZnB_2O_7$ is qualitatively consistent with the presence of a larger concentration of the heavy and polarizable Bi^{3+} cations in its crystal structure. As has been shown by theoretical calculations in the case of BiB_3O_6,[7] the asymmetric BiO_n coordination polyhedra are major contributors to the SHG efficiency of bismuth borates. The BiO_6 polyhedra in $Bi_2ZnB_2O_7$ (Figure 2a, Table 5) are indeed significantly more asymmetric than the BiO_8 polyhedra in $CaBiGaB_2O_7$ (Figure 3a, Table 6), thus leading to a reduced cancellation of the Bi−O bond polarizabilities and a larger nonlinear optical (NLO) activity in the former. Moreover, according to the anionic group theory of NLO activity in borates,[34,35] the contribution to the SHG efficiency of the borate groups can also be qualitatively predicted to be larger in $Bi_2ZnB_2O_7$ due to the presence of planar BO_3 groups in the B_2O_5 dimers (although the dimers themselves are not planar but twisted by about 48° around the bridging O atom, Figure 2b). By comparison, the nonplanar tetrahedral BO_4 groups in the B_2O_7 dimers of $CaBiGaB_2O_7$ would contribute less to the SHG efficiency. Efforts are currently underway to grow large single crystals of $Bi_2ZnB_2O_7$ in order to measure a more complete set of NLO properties. Preliminary Czochralski and flux growth experiments using Bi_2O_3-rich melts show promising results toward this goal.

Conclusion

The borates described in this work, $Bi_2ZnB_2O_7$, $CaBiGaB_2O_7$, and $CdBiGaB_2O_7$, are the only examples of synthetic diborate members of the melilite family, $A_2XZ_2O_7$. They are also the only examples of melilites containing the Bi^{3+} cation. Whereas $CaBiGaB_2O_7$ and $CdBiGaB_2O_7$ crystallize with the normal tetragonal melilite structure ($P\bar{4}2_1m$ symmetry, $Z = 2$), $Bi_2ZnB_2O_7$ adopts a unique orthorhombic superstructure of melilite ($Pba2$ symmetry, $Z = 4$). The structural analysis has established that the lower symmetry and the larger unit cell of $Bi_2ZnB_2O_7$ result from the stereoactive lone pairs of the Bi^{3+} cations. In particular, the

(34) Chen, C.; Wu, Y.; Jiang, A.; Wu, B.; You, G.; Li, R.; Lin, S. *J. Opt. Soc. Am. B* **1989**, *6*, 616.

(35) Becker, P. *Adv. Mater.* **1998**, *10*, 979.

strongly asymmetric coordination environment of Bi^{3+} leads to the formation of B_2O_5 diborate groups not previously encountered in the melilite family. The preliminary measurement of the efficiency for second harmonic generation of $Bi_2ZnB_2O_7$ powder has shown promising results that will be explored further with more detailed measurements on large single crystals.

Acknowledgment. Part of this work was supported by a discovery grant to J.B. from the Natural Sciences and Engineering Research Council of Canada. Access to the C2 neutron powder diffractometer maintained by the National Research Council of Canada at the Chalk River Laboratories is gratefully acknowledged. The preliminary measurements of nonlinear optical properties were carried out in Professor Vargas-Baca's laboratory at McMaster University.

Supporting Information Available: Indexed X-ray powder diffraction patterns for $Bi_2ZnB_2O_7$ (Table 7), $CaBiGaB_2O_7$ (Table 8), and $CdBiGaB_2O_7$ (Table 9) (PDF) and the full Rietveld refinement profiles for $Bi_2ZnB_2O_7$ and $CaBiGaB_2O_7$ (Figures 1a and 1b) (TIFF). This material is available free of charge via the Internet at http://pubs.acs.org.

CM0503073